Journal of Renewable Materials

Tech Science Press

DOI: 10.32604/jrm.2021.012885

ARTICLE

Prediction and Analysis of Post-Treatment of Sustainable Walnut Shell/Co-PES Parts by Laser Sintering

Yueqiang Yu[1], Suling Wang[1,*], Minzheng Jiang[1], Yanling Guo[2,3] and Ting Jiang[1,*]

[1]Northeast Petroleum University, College of Mechanical Science and Engineering, Daqing, 163318, China

[2]Northeast Forestry University, College of Mechanical and Electrical Engineering, Harbin, 150040, China

[3]Northeast Forestry University, Research and Development Center of 3D Printing Material and Technology, Harbin, 150040, China

[*]Corresponding Authors: Suling Wang. Email: wangsuling@nepu.edu.cn; Ting Jiang. Email: jiangting1112@163.com

Received: 16 July 2020 Accepted: 27 August 2020

ABSTRACT

In order to enhance the strength of sustainable walnut shell/Co-PES (WSPC) sintered parts, wax-filtrated post-treatment was carried out. The effects of treating fluid temperature, preheating time and immersion time on the bending strength of WSPC wax-filtrated parts were analyzed by single factor analysis method. To obtain an accurate model for predicting the bending strength of the WSPC wax-filtrated part, the experiments were involved by using Box-Behnken design (BBD). Main parameters, such as treating fluid temperature, preheating time and immersion time, and their interactive effects were analyzed through analysis of variance (ANOVA) and graphical contours. The results demonstrated that all parameters' direct effects were significant to bending strength of the WSPC wax-filtrated part. Its optimum value was 5.0 MPa when the treating fluid temperature of 70°C, preheating time of 50 min, and immersion time of 20 s. The predicted models effectively validated had good predicting accuracy. The WSPC wax-filtrated part using optimal processing parameters was processed by investment casting, and then the metal casting of dimensional stability and smooth surface was obtained. Investment casting was done using WSPC wax-filtrated parts under optimal process parameters and then metal parts with stable structure size and smooth surface can be obtained, which indicates that WSPC material can be used for investment casting.

KEYWORDS

Agricultural and forestry wastes; three-dimensional printing; selective laser sintering; post processing; response surface methodology

1 Introduction

Selective Laser Sintering (SLS), a 3D printing technology, was proposed by the Decker [1]. Compared with traditional techniques, SLS can effectively fabricate parts of small volume and structural diversity. Furthermore, SLS has some strengths over other 3D printing techniques, for instance, materials can be reused and high-precision parts can be fabricated [2,3]. Therefore, SLS has been widely used in aerospace, automobile manufacturing, medical treatment, and casting [4–7].

In recent years, the materials mostly concentrate on ceramics, metals, polymers and their composites in SLS [8–14]. Polymer was firstly applied in SLS, however, it has not widely used due to its high price, high demand of machining conditions, and big warping deformation. Interestingly, biomass composites are new materials for SLS because of low energy consumption, environmental protection and sustainability. They are mixtures including biomass material as raw material, such as the wood powder, bamboo powder, rice husk, walnut shell powder, and polymer material, as well as trace of additives mixed by mechanical mixing method [15–20]. Biomass composites have advantages such as low cost, simple preparation process and good forming performance. Therefore, sintering parts consisting of biomass composites can be used in some fields such as product design, automotive interior, investment casting and water treatment [21,22]. There are some defects such as high porosity and low mechanical strength, though these parts have high forming accuracy and complex structure. Therefore, it is necessary to study the post-processing of SLS sintering parts of biomass composites to improve their internal defects and mechanical properties.

Walnut shell is often abandoned as agricultural waste [23]. However, walnut shell powder has unique advantages (easy crushing and wide availability), compared to wood, bamboo, rice husk [16,24,25]. In addition, walnut shell powder of different particles diameters can be obtained without large and complex equipment, so that it is easy to meet the requirements of powder particle size of material by SLS. Walnut shell powder particle was approximately spherical [18]. In SLS, walnut shell contributes to the spreading and dispersion of powder because of its nearly spherical powder particles. It is helpful to obtain high-precision parts. Besides, the porous and good absorptive walnut shell powder particles are easily permeated with molten copolyester hot melt adhesive (Co-PES) powder and treatment fluid, which can improve the inner defect and mechanical property of the walnut shell/Co-PES composite (WSPC) parts [26]. Therefore, this study used walnut shell powder as the raw material to prepare WSPC parts and WSPC post-processing parts. But in the process of post processing, there are many influence factors. Therefore, how to balance the relationship between various factors and gain the optimized process parameters of the optimum mechanical properties of WSPC wax-filtrated part is very important. Response surface methodology (RSM), also known as the regression design, can obtain the best combination of factor levels through establishing surface model of continuous variable, and finding out quantitative rules between test indexes and various factors. Compared to the design method of single factor experiment and orthogonal experiment design method, RSM is more reasonable, for example, it can determine the best value of the test results as well as fit the obtained simulation equation and real value.

At present, studies on optimization of post-processing process of WSPC parts by response surface analysis (RSM) have not been reported in the literature. Therefore, in our research, SLS technology was used to manufacture WSPC parts and post-processing parts. Evaporative pattern casting (EPC) needs to have enough strength and toughness to avoid rupture and deformation in the process of production operation and storage. Hence, it is necessary to discuss the influence of processing parameters of post processing on the bending strength of WSPC wax-filtrated part. On the basis of single factor, the Box-Behnken design (BBD) was used to examine the influence of single effect and interactive effects of treating fluid temperature, preheating time and immersion time on the bending strength of WSPC wax-filtrated part. Additionally, the predicted models were established, and then optimal process parameters were obtained. The WSPC wax-filtrated part using optimal processing parameters was processed by investment casting, and then the metal casting of dimensional stability and smooth surface was obtained.

2 Materials and Methods

2.1 Materials and Preparation of WSPC Powder

Walnut shell powder was bought from Ding Sheng Corundum Abrasives Ltd. in China. Its characteristic is as follows: nearly spherical porous particles, apparent density of 0.48 g cm^{-3}, particle diameter of 58–96 μm. Co-PES powder was obtained by Shanghai Tiannian Material Technology Ltd. It is smooth-surfaced white

block particle, apparent density of 0.7 g cm^{-3}, particle diameter of 0–58 μm. Lubricant was provided from Tianjin Guangfu Fine Research Institution. Its melting point is 125°C and zinc stearate density is 1.095 g cm^{-3}. Light stabilizers were from Zhenhai Jianghua Chemical Industry Ltd. Its melting point is 80°C and density is 1.18 g cm^{-3}.

WSPC powder was mainly made of walnut shell powder, Co-PES powder and micro-additive. Before WSPC powder was prepared, walnut shell powder was dehydrated at a temperature of 105°C for 3.5 h in DHG-9146A incubator from Shanghai Jinghong Experimental Equipment Co., Ltd. in China. Walnut shell powder was weighed every 1 h until the mass remained unchanged. Then, WSPC powder was prepared from mixing the dried walnut shell powder, Co-PES powder and micro-additive by mechanical mixing method [26].

2.2 Process Principle of SLS

Through an AFS-360 rapid prototyping equipment from Beijing Longyuan Technology Ltd. in China, SLS experiments were processed. Fig. 1a shows the process state. Tab. 1 shows optimized processing parameters of SLS [27]. The equipment mainly composed of powder spreading system, laser scanning system, working cylinder, heat control system, and CO_2 laser generator (laser power of 55 W and wavelength of 10.6 μm). Based on the CAD model, through repeatedly depositing a thin layer of fusible powder and selectively sintering each layer to the next layer with a modulated laser beam, in a repetitive manner, and then a three-dimensional solid object is obtained. The schematic diagram of process is displayed in Fig. 1b.

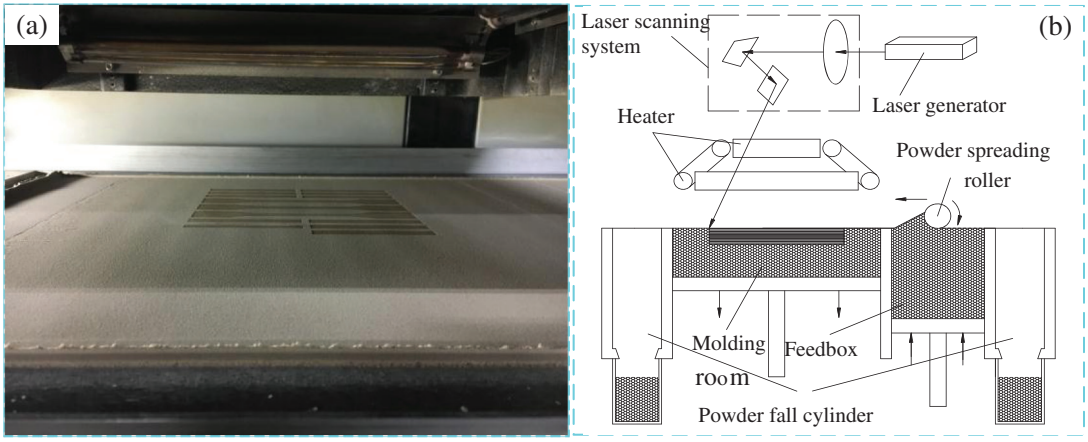

Figure 1: Experiment of selective laser sintering (SLS) and schematic diagram of process: (a) processing state; (b) schematic diagram of process

Table 1: The processing parameters of walnut shell/Co-PES powder composites (WSPC)

Laser Power (W)	Scan Speed (mm/s)	Layer Thickness (mm)	Scan Spacing (mm)	Preheating Temperature (°C)	Processing Temperature (°C)
12	2000	0.15	0.2	80	75

2.3 Post Processing and Treatment Fluid

Industrial wax: No. 3 light stability, oil addition of 0.32%, melting point of 58.58°C, kinematic viscosity of 3.786 mm^2 s^{-1}. Stearic acid: density of 0.94 g cm^{-3}, melting point of 69.6°C, boiling point of 232°C, flashing point of 220.6°C.

Clean up the WSPC parts and then put them into the incubator at a temperature of 60°C and the heat was kept unchanged for some time. The stearic acid and industrial wax were blended as 1:1 ratio by mass. The WSPC parts were removed from the incubator when the temperature stayed unchanged, and then immersed in the melted treatment fluid for a while. They were left to room temperature after removing in order to obtain the wax-filtrated parts. Fig. 2 shows the flow chart of wax filtrated post processing of WSPC parts.

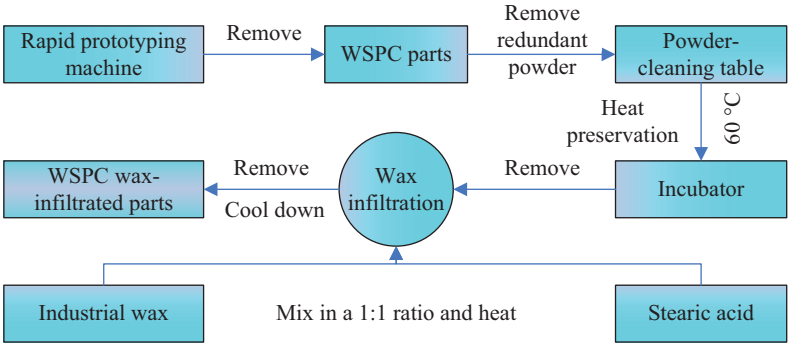

Figure 2: The flow chart of post processing of WSPC parts

2.4 Post Processing and Treatment Fluid

Scanning electronic microscopy (SEM): The test was conducted using a FEI Quanta200 SEM produced by the Dutch company (Amsterdam, Netherlands). The surfaces and cross-sections of WSPC parts and the optimized WSPC wax-filtrated parts were sputtered with gold first because specimens were non-conductive. The SEM figures of their morphologies were obtained.

Mechanical test: Bending strength of WSPC wax-filtrated parts were tested using a CMT5504 universal tensile tester of MTS System Ltd. (Minnesota, America). Span length is 64 mm and crosshead speed is 5 mm min^{-1}.

Thermogravimetric analysis (TG): the test was conducted using a Pyris 6 thermogravimetric analyzer of Perkin Elmer company (America). The mass of optimized WSPC wax-filtrated parts was 10 mg; the testing was performed using nitrogen atmosphere, temperature range was 40–600°C and heating rate was 10°C min^{-1}. TG curves of the optimized WSPC wax-filtrated parts were obtained.

3 Design of Experiments

3.1 Single Factor Experimental Design

The post processing experiment of WSPC parts demonstrated that treating fluid temperature, preheating time, and immersion time were the most relevant parameters on the WSPC wax-filtrated part. The parameters' variation range should be firstly defined to ensure the feasibility of RSM experimental design. Tab. 2 shows post processing process parameters of WSPC parts.

Table 2: The processing parameters of post processing of single factor

Factors	Preheating time (min)	Treating fluid temperature (°C)	Immersion time (s)
A1/A2/A3/A4/A5	20/30/40/50/60	70	30
B1/B2/B3/B4/B5	30	65/70/75/80/85	30
C1/C2/C3/C4/C5	30	70	10/20/30/40/50

3.2 RSM Experimental Design

On the basis of single factor experiment of post processing of WSPC parts, three main factors were defined. In the BBD experiment, preheating time (x_1), treating fluid temperature (x_2), and immersion time (x_3) as input parameters were set to three levels. The bending strength of WSPC wax-filtrated part (Y) was set as output parameter. Tab. 3 shows the input parameters and the corresponding levels.

Table 3: The factors and levels used in Box-Behnken design (BBD)

Levels	Factors		
	x_1: Preheating time (min)	x_2: Treating fluid temperature (°C)	x_3: Immersion time (s)
−1	40	65	10
0	50	70	20
1	60	75	30

The fitted response equation of bending strength with least squares is given by:

$$Y = B_0 + B_1x_1 + B_2x_2 + B_3x_3 + B_{11}x_1^2 + B_{22}x_2^2 + B_{33}x_3^2 + B_{12}x_1x_2 + B_{13}x_1x_3 + B_{23}x_2x_3 \quad (3.1)$$

where Y is output parameter; B_0 represents constant term; B_1, B_2, B_3 stand for linear coefficients; B_{12}, B_{13}, B_{23} denote interaction coefficients; B_{11}, B_{22}, B_{33} express coefficients of quadratic term; x_1, x_2, x_3 stand for input parameters.

4 Results and Discussion

4.1 Single Factor Experiment

Fig. 3 presents the influence of different factors on the bending strength of WSPC wax-filtrated parts. The WSPC wax-filtrated specimens after bending strength test are seen in Fig. 3a. Fig. 3b illustrates the effect of preheating time on the bending strength of WSPC wax-filtrated parts. It was demonstrated that the bending strength of WSPC wax-filtrated parts increase with the increase of preheating time when the preheating time increased from 20 min to 50 min. However, when preheating time is longer than 50 min, bending strength of WSPC wax-filtrated parts decreased with increasing of preheating time. The preheating time can affect inner temperature distribution and structure of forming part. The short preheating time leads to high external temperature of forming part, low internal temperature, external thermal expansion and pore expansion, which promotes the treatment fluid penetration. Low internal temperature results in poor treatment liquid fluidity and incomplete treatment liquid penetration, thus reducing the bending strength of wax-filtrated parts. The long preheating time causes aging of the forming part and damage to the internal structure of the forming part, thus reducing the bending strength

of the wax-filtrated parts. Therefore, the optimum range of preheating time affecting WSPC wax-filtrated parts was 40–60 min.

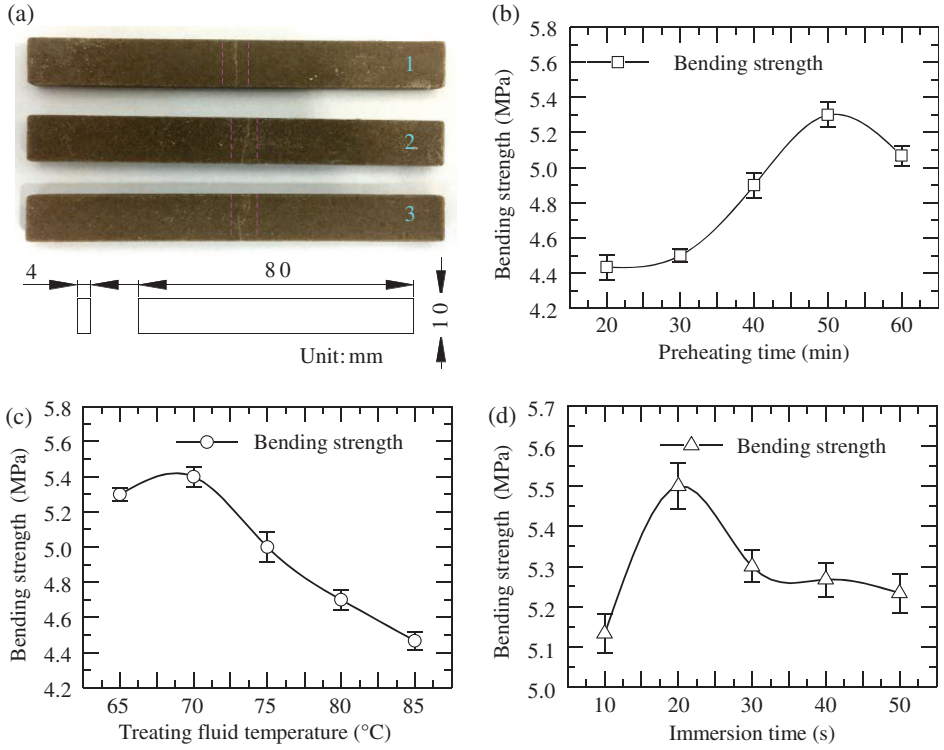

Figure 3: The curves of bending strength with different effect factors: (a) bending specimen; (b) preheating time; (c) treating fluid temperature; (d) immersion time

The influence of treatment fluid temperature on the bending strength of WSPC wax-filtrated parts is observed in Fig. 3c. It can be seen that when treatment fluid temperature was 65–70°C, the bending strength of WSPC wax-filtrated parts increased continually with increasing of treatment fluid temperature. However, when treatment fluid temperature was 70–85°C, bending strength of WSPC wax-filtrated parts decreased gradually with increasing of treatment fluid temperature. The treatment fluid can affect inner filtration effect and inner structure of forming part. The low temperature of the treatment fluid and insufficient infiltration force result in the outside part being infiltrated, while the inside part is not infiltrated and there were many pores. With the increase of the temperature of the treated fluid, the wetting force was strengthened, and the wetting effect was improved, thus increasing the bending strength of the wax-filtrated parts. However, the high temperature of the treatment liquid destroys the internal structure of the forming parts, thus reducing the bending strength of the wax-filtrated parts. Hence, the optimum range of treatment fluid temperature on the bending strength of WSPC wax-filtrated parts was 65–75°C.

Fig. 3d shows the influence of immersion time on the bending strength of WSPC wax-filtrated parts. When the immersion time was 10–20 s, the bending strength of WSPC wax-filtrated parts increased continually with increasing of immersion time. However, as immersion time was 20–50 s, bending strength of WSPC wax-filtrated parts decreased gradually with increasing of immersion time. The immersion time can affect filtration effect and inner structure of forming part. The short immersion time makes the outer structure of the forming part filled with the treatment fluid, while the inner structure has

not been incompletely filled by the treatment fluid, thus reducing the bending strength of the wax-filtrated part. The long immersion time causes damage to the internal structure of the forming part, thus reducing the bending strength of the wax-filtrated parts. Therefore, the optimum range of immersion time on the bending strength of WSPC wax-filtrated parts was 10–30 s.

Overall, the optimum range of factors on the bending strength of WSPC wax-filtrated parts: preheating time of 40–60 min, treatment fluid temperature of 65–75°C, the immersion time of 10–30 s.

4.2 RSM Experiment

4.2.1 Multiple Regression Model and Analysis of Variance

Tab. 4 shows the process parameters as well as their corresponding codes and levels. In this study, RSM using a BBD was applied. It is well-known that RSM can effectively save experimental cost and time. Only 12 unique combinations were chosen, and extra 5 repeated tests were added for the process parameters. Three repeated tests were conducted every run and then the average value was obtained.

Table 4: The BBD and results

Serial number	Preheating time (min)	Treating fluid temperature (°C)	Immersion time (s)	Bending strength (MPa)
1	0	1	−1	3.70
2	1	0	1	4.50
3	−1	1	0	3.67
4	0	1	1	3.75
5	1	−1	0	3.90
6	0	−1	1	4.30
7	0	−1	−1	3.85
8	1	1	0	3.80
9	0	0	0	4.85
10	0	0	0	4.63
11	1	0	−1	4.00
12	0	0	0	4.60
13	0	0	0	4.70
14	−1	0	1	4.45
15	−1	0	−1	4.40
16	0	0	0	4.70
17	−1	−1	0	4.35

The experiment plan was developed by Version 8.0.6 of the Design-Expert Software, and the experimental data were also analyzed using this software. The data in Tab. 4 was processed by multiple regression fit. The binary multiple regression model for response value was established.

$$R_1 = 4.70 - 0.084x_1 - 0.18x_2 + 0.13x_3 + 0.14x_1x_2 + 0.11x_1x_3 - 0.100x_2x_3 - 0.16x_1^2 - 0.60x_2^2 - 0.19x_3^2 \quad (4.1)$$

where R_1 is response value; x_1 is preheating temperature; x_2 is treatment fluid temperature; x_3 is immersion time.

In order to evaluate the reliability of test results and models, the results of each parameter evaluated by analysis of variance (ANOVA) and significance test are shown in Tabs. 5 and 6. Tab. 5 shows that The regression of this model is significant ($P < 0.0001$), namely, the treating fluid temperature, preheating time, and immersion time had significant influences on responses obviously, and their interaction was also obvious. Tab. 6 shows that coefficient of determination was 0.9852 and coefficient of adjusted determination was 0.9662. It meant that this model can explain the change of 98.52% of response values. It indicated that the degree of fitting is good and the error is small. Therefore, the models applied to analyze and predict the bending strength of WSPC wax-filtrated parts is feasible.

Table 5: Analysis of variance (ANOVA) for regression models

Source	Sum of squares	Degree of freedom	Mean square	*F*-value	*P*-value
Model	2.570	9	0.290	51.79	<0.0001
x_1	0.056	1	0.056	10.19	0.0152
x_2	0.270	1	0.270	49.72	0.0002
x_3	0.140	1	0.140	25.03	0.0016
x_1x_2	0.084	1	0.084	15.27	0.0058
x_1x_3	0.051	1	0.051	9.19	0.0191
x_2x_3	0.040	1	0.040	7.26	0.0309
x_{12}	0.110	1	0.110	20.63	0.0027
x_{22}	1.520	1	1.520	276.88	<0.0001
x_{32}	0.160	1	0.160	28.85	0.0010
Residual	0.039	7	0.0055		
Lack of fit	0.0012	3	0.0004	0.044	0.986
Error	0.037	4	0.0093		
Sum	2.610	16			

Table 6: Analysis of model

Responses	Standard Deviation	Mean Value	Dispersion Coefficient	R^2	Adjusted R^2
Result	0.074	4.24	1.75	0.9852	0.9662

The relationships between the predicted values and actual values of bending strength of WSPC wax-filtrated parts are shown in Fig. 4. The results were uniformly distributed around a straight line in a narrow range. The normal probabilities of the residual values were also confirmed by the straight line. The agreement of predicted values and the actual values was obvious. The fitted models had a good approximation for those independent variables.

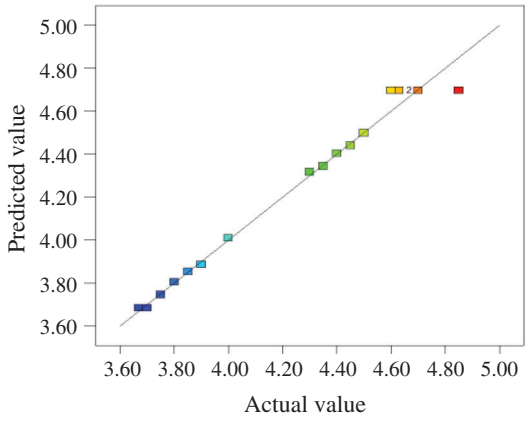

Figure 4: The relationship between predicted value and actual value of bending strength of wax-filtrated part

4.2.2 Experiment Result of RSM

Response surface and contour graphs of the relationship between the preheating time, treatment fluid temperature and immersion time are plotted through the regression equation, as shown in Fig. 5.

From Fig. 5a, it can be seen that response surface is in bending state, and response surface bending degree is big along the direction of treatment fluid temperature, and its bending degree is small along the direction of preheating time. In Fig. 5b, it is clear that contour is elliptical, and the center of ellipse is the peak of the bending strength of WSPC wax-filtrated parts. Contour is dense along the direction of treatment liquid temperature; contour is scattered along the direction of preheating time. Hence, the influences of the preheating time and treatment fluid temperature on the WSPC permeability wax the bending strength are significant, but the influence of treatment fluid temperature on the bending strength of WSPC wax-filtrated parts is more significant than that of preheating time.

From Fig. 5c, the response surface is in bending state, and response surface bending degree is small along the direction of preheating time and immersion time. In Fig. 5d, it is clear that contour is elliptical, and the center of ellipse is the peak of the bending strength of WSPC wax-filtrated parts. Contour is scattered along the direction of both preheating time and immersion time. Therefore, the influences of preheating time and immersion time on the WSPC permeability wax the bending strength are significant.

From Fig. 5e, it can be clear that response surface is in bending state, and response surface bending degree is big along the direction of treatment fluid temperature, and its bending degree is small along the direction of immersion time. In Fig. 5f, it is clear that contour is elliptical, and the center of ellipse is the peak of the bending strength of WSPC wax-filtrated parts. Contour is dense along the direction of treatment liquid temperature; contour is scattered along the direction of immersion time. Hence, the immersion time and treatment fluid temperature on the WSPC permeability wax the influences of the bending strength are significant, but the influence of treatment fluid temperature on the bending strength of WSPC wax-filtrated parts is more significant than that of immersion time.

The optimal processing parameter of post processing of WSPC part was developed by Version 8.0.6 of the Design-Expert Software, which shows that bending strength of the WSPC wax-filtrated part was optimum value was 5.0 MPa as treating fluid temperature of 70°C, preheating time of 50 min, immersion time of 20 s. The optimal processing parameters is just the parameters at 5 repeated tests. The bending strength was 4.7 MPa using optimum parameters. The value shows close approximation to the predicted value, which indicates that the degree of fitting is good.

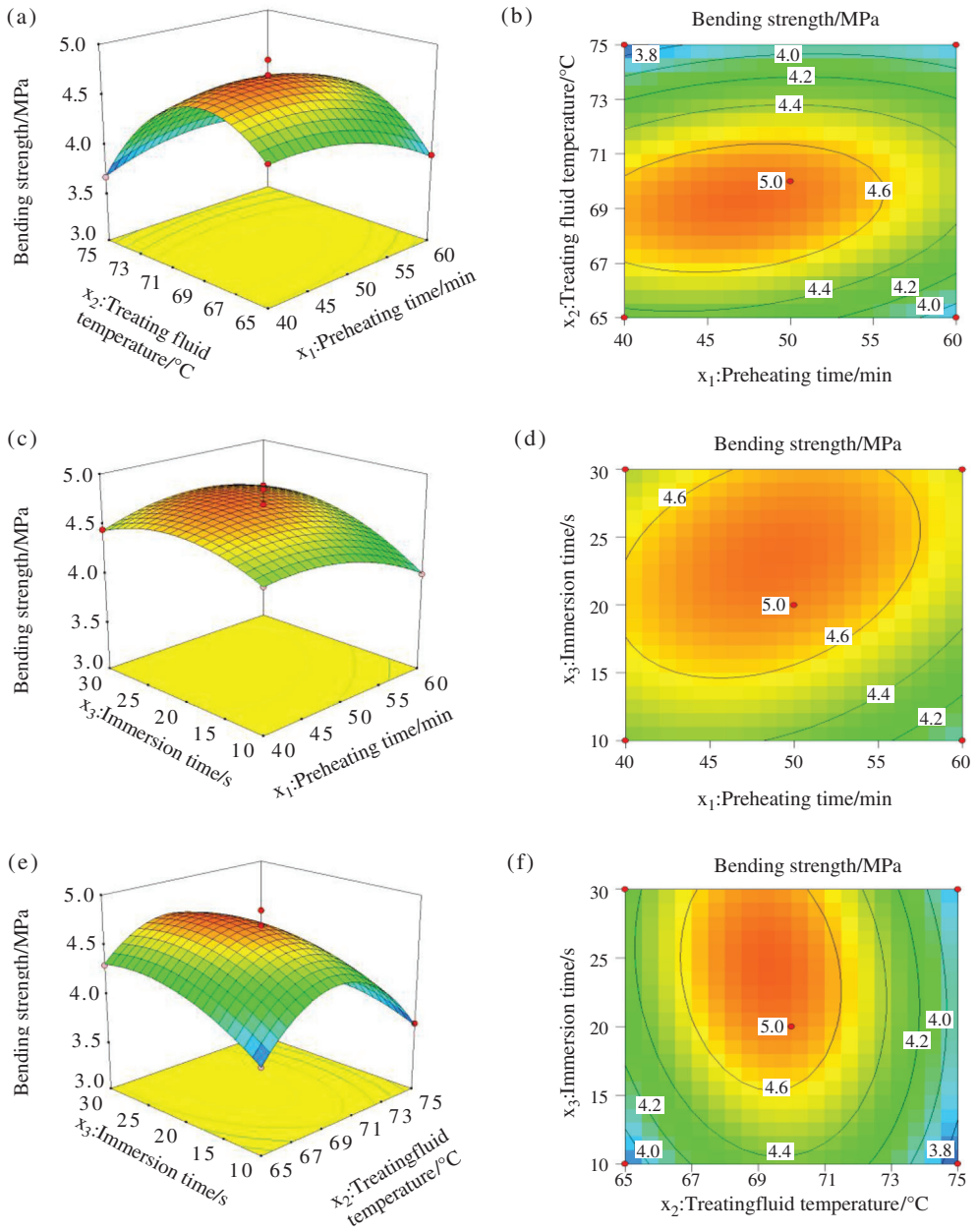

Figure 5: Response surface and contour graphs of bending strength of wax-filtrated part: (a)–(b) Preheating time and treatment fluid temperature; (c)–(d) Preheating time and immersion time; (e)–(f) Treatment fluid temperature and immersion time

4.3 Morphologies

The SEM images of the surfaces and cross-sections of WSPC parts and the optimized WSPC wax-filtrated parts are shown in Fig. 6. Figs. 6a and 6b show that although high temperature can accelerate the spread of the powder, forming sintered parts of a large number of sintering neck and low porosity [28], but because of the walnut shell powder particle hinders the laser beam to Co-PES powder particles and the flow of molten Co-PES fluid, only forming the smaller sintering neck on the surface of WSPC sintering, not a large continuous sintering zone, so there are a large number of holes and pores on the

surface and inside of the WSPC parts, which affects surface quality and mechanical properties of WSPC parts. However, wax-filtrated post-treatment can effectively improve the surface and internal structure of WSPC parts, and the larger the surface cavity and internal pores of the parts are, the more conducive to the post-treatment fluid infiltration, but too large pores and holes are not conducive to the full filling of the post-treatment fluid. Figs. 6c and 6d show the morphologies of surface and cross-section of the optimized WSPC wax-filtrated parts. Fig. 6c shows that through wax-filtrated treatment of WSPC parts, the holes on the surface of WSPC parts are almost immersed by treatment fluid, thus filling the surface up. Therefore, the surface quality of WSPC parts is improved. Fig. 6d shows that after wax-filtrated treatment, because a large number of air in WSPC parts, and wax-filtrated treatment technology is under natural conditions, air can not to be completely vented, causing a small amount of porosity inside the parts, but most internal pores of WSPC parts is filled, so as to effectively improve the internal structure of WSPC parts. Hence, the surface quality and mechanical property of WSPC parts become better by wax-filtrated treatment.

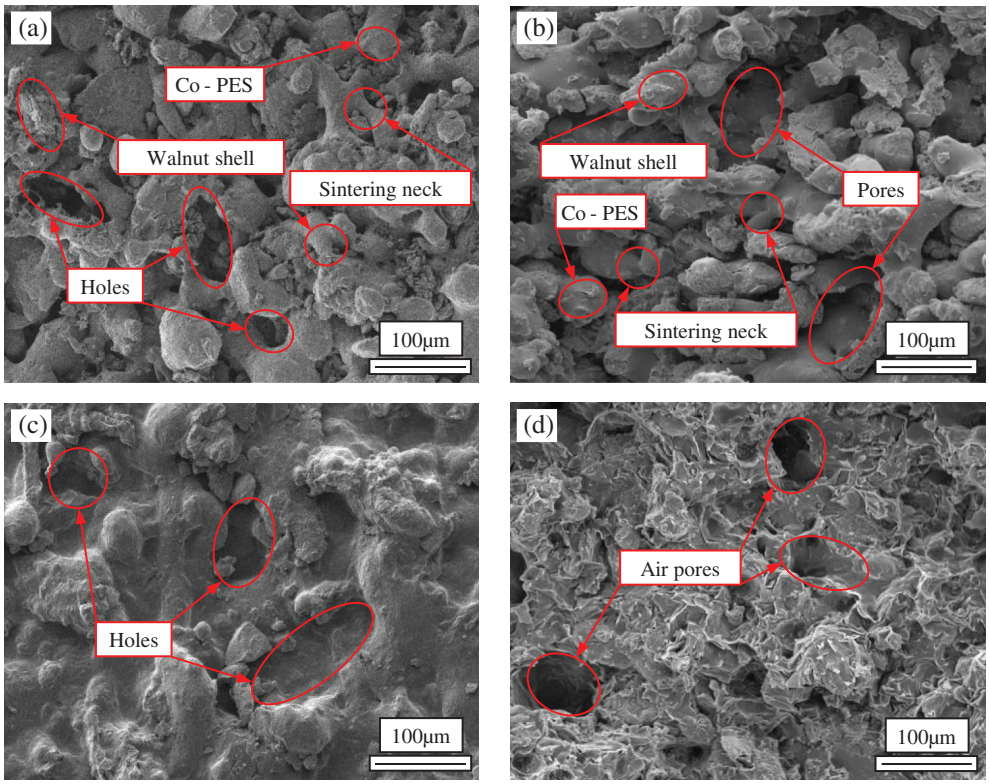

Figure 6: Scanning electronic microscopy (SEM) images of the surfaces and cross-sections of WSPC parts and the optimized WSPC wax-infiltrated parts: (a) surface of WSPC part; (b) cross-sections of WSPC part; (c) surface of WSPC wax-infiltrated part; (d) cross-section of WSPC wax-infiltrated parts

4.4 Investment Casting

Fig. 7 shows the investment casting process of WSPC part. In Fig. 7a, WSPC part of stable shape dimension, clear outline and smooth surface is observed. But it is inevitable that there is obvious staircase effect only in curved surface of the local part, which is the characteristic of selective laser sintering technology. Staircase effect tends to affect surface quality of the curved surface of the part, but through the post-treatment process and surface treatment process, the curved surface quality defects generated

from the staircase effect can be mended (see Fig. 7b), so as to improve the surface quality of WSPC wax-filtrated part.

According to the flow chart of investment casting process, optimized WSPC wax-filtrated part was used for investment casting. WSPC wax-filtrated part was processed by smearing refractory materials, stucco, and hardening to prepare a mould cavity. Then the mould cavity was processed by dewaxing under high temperature of 150–160°C and high pressure of 5–6 MPa for 1 h. The temperature rose to approximately 850–100°C and heat was preserved for 2 h, and then dropped to 300°C for roasting. TG results was observed in Fig. 7c. The decomposition temperature of WSPC wax-infiltrated parts was 211.86°C, the maximum weight loss rate temperature was 278.77°C, the termination decomposition temperature was 600°C, and the residual mass after decomposition accounts for 13.155% of the total mass, where the residual mass was ash mass, so the ash content of WSPC wax-infiltrated parts was large. WSPC wax-filtrated part contained a large number of ash. In order to avoid the ash content influencing quality of casting, after roasting, the residues of WSPC parts were removed by high-press air. Finally, molten steel was poured into the mould after preheating to 900°C. The metal casting was obtained after treatment such as polishing and sanding. Experimental results showed that metal casting part was of stable structure and smooth surface (Fig. 7d). The surface quality of investment casting was not affected by staircase effect of WSPC parts and residues. The result showed that EPC fabricated by SLS WSPC powder not only produces parts of complex structure, but also produces metal casting effectively.

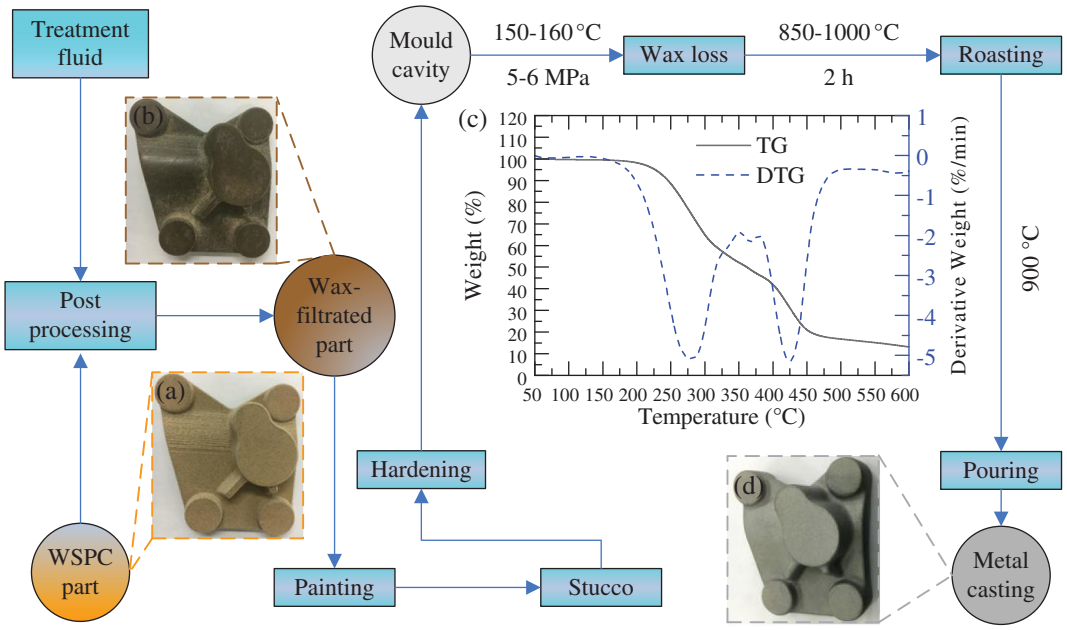

Figure 7: Investment casting process of WSPC part: (a) WSPC part; (b) optimized WSPC wax-infiltrated part; (c) TG and DTG curves of optimized WSPC wax-infiltrated part; (d) metal casting part

5 Conclusions

In this paper, the effect of post-processing parameters on the mechanical strength of WSPC wax-filtrated part was obtained. The impacts of treating fluid temperature, preheating time, and immersion time on the bending strength of WSPC wax-filtrated parts were analyzed by single factor analysis method. The results showed that the optimum range of effect factors were the treating fluid temperature of 65–75°C, preheating time of 40–60 min and immersion time of 10 MPa. In addition, the processing parameters of

post processing were optimized using RSM, which showed that bending strength of the WSPC wax-filtrated part was optimum value was 5.0 MPa as treating fluid temperature of 70°C, preheating time of 50 min and immersion time of 20 s. Through tests, bending strength of the WSPC wax-filtrated part was 4.7 MPa using optimum parameters. Test value was closed to predicted value, which illustrated that the process parameters' selection consideration was derived from the desirability function by RSM. The WSPC wax-filtrated part using optimal processing parameters was processed by investment casting, and then the metal casting of dimensional stability and smooth surface was obtained. The result showed that EPC was fabricated by SLS WSPC powder, which meets the requirement for a fast changing market and single and small batch production.

Funding Statement: This study was supported by Scientific Research Staring Foundation of Northeast Petroleum University (1305021868), the National Natural Science Foundation of China (51475089), the National Key R&D Program of China (2017YFD0601004), the Natural Science Foundation of Heilongjiang Province (ZD2017009), Fundamental Research Funds for the Central Universities (2572017PZ06) and the Special Project of Scientific and Technological Development of Central Guidance for Local (ZY16C03).

Conflicts of Interest: The authors declare that they have no conflicts of interest to report regarding the present study.

References

1. Deckard, C. R. (1988). *Selective laser sintering (Ph.D. Thesis)*. The University of Texas at Austin, USA.
2. Ligon, S. C., Liska, R., Stampfl, J., Gurr, M., Mülhaupt, R. (2017). Polymers for 3D printing and customized additive manufacturing. *Chemical Reviews, 117,* 10212–10290. DOI 10.1021/asc.chemrev.7b00074.
3. Wang, X., Jiang, M., Zhou, Z., Gou, J. H., Hui, D. (2017). 3D printing of polymer matrix composites: a review and prospective. *Composites Part B: Engineering, 110,* 442–458. DOI 10.1016/j.compositesb.2016.11.034.
4. Jiang, Z. J., Wang, R. D., Lv, C. J., Zhang, M., Li, L. X. (2018). 3D printing technology in the development of automobile inside and outside trim parts for application. *Automobile Applied Technology,* 91–93. DOI 10.16638/j.cnki.1671-7988.2018.05.029.
5. Rokicki, P., Kozik, B., Budzik, G., Dziubek, T., Bernaczek, J. et al. (2016). Manufacturing of aircraft engine transmission gear with SLS (DMLS) method. *Aircraft Engineering & Aerospace Technology, 88(3),* 397–403. DOI 10.1108/AEAT-05-2015-0137.
6. Chen, T. T., Liu, J. X., Shi, F. X., Wang, Y. M., Zheng, B. R. (2016). Casting technology of combining 3D print with vacuum pressurizing for engine cylinder head samples. *Foundry Technology, 37,* 582–584. DOI 10.16410/j.issn1000-8365.2016.03.049.
7. Du, Y., Liu, H., Yang, Q., Wang, S., Wang, J. L. et al. (2017). Selective laser sintering scaffold with hierarchical architecture and gradient composition for osteochondral repair in rabbits. *Biomaterials, 137,* 37–48. DOI 10.1016/j.biomaterials.2017.05.021.
8. Bourell, D. L. (2016). Sintering in laser sintering. *JOM Journal of the Minerals Metals & Materials Society, 68(3),* 885–889. DOI 10.1007/s11837-015-1780-2.
9. Almangour, B., Grzesiak, D., Yang, J. M. (2017). Scanning strategies for texture and anisotropy tailoring during selective laser melting of TiC/316L stainless steel nanocomposites. *Journal of Alloys & Compounds, 728,* 424–435. DOI 10.1016/j.jallcom.2017.08.022.
10. Chang, S., Li, L. Q., Lu, L., Fuh, J. Y. H. (2017). Selective laser sintering of porous silica enabled by carbon additive. *Materials, 10(11),* 1313. DOI 10.3390/ma10111313.
11. Salmoria, G. V., Lauth, V. R., Cardenuto, M. R., Magnago, R. F. (2017). Characterization of PA12/PBT specimens prepared by Selective Laser Sintering. *Optics & Laser Technology, 98,* 92–96. DOI 10.1016/j.optlastec.2017.07.044.

12. Guo, J., Bai, J. M., Liu, K., Wei, J. (2018). Surface quality improvement of selective laser sintered polyamide 12 by precision grinding and magnetic field-assisted finishing. *Materials & Design, 138,* 39–45. DOI 10.1016/j.matdes.2017.10.048.
13. Warnakula, A., Singamneni, S. (2017). Selective laser sintering of nano Al_2O_3 infused polyamide. *Materials, 10 (8),* 864. DOI 10.3390/ma10080864.
14. Zhou, P., Qi, H. L., Zhu, Z. Y., Qin, H., Li, H. et al. (2012). Development of *SiC*/PVB composite powders for selective laser sintering additive manufacturing of *SiC*. *Materials, 11,* 2012. DOI 10.3390/ma11102012.
15. Guo, Y. L., Jiang, K. Y., Yu, Z. X., Xin, Z. S., Zeng, W. L. (2011). The preparation technology and forming properties of wood-plastic composite powder used in selective laser sintering. *Journal of Shanghai Jiaotong University, 45,* 1327–13311.
16. Zeng, W. L., Guo, Y. L., Jiang, K. Y., Yu, Z. X., Liu, Y. (2012). Preparation and selective laser sintering of rice husk-plastic composite powder and post treating. *Journal of Nanomaterials and Biostructures, 7,* 1063–1070. DOI 10.4028/www.scientific.net/KEM.667.320.
17. Zhao, D. J., Guo, Y. L., Song, W. L., Jiang, K. Y. (2015). Preparation and forming characteristics of bamboo powder/co-polyamide laser sintering composite materials. *Journal of Northeast Forestry University, 43,* 107–109, 115. DOI 10.4028/www.scientific.net/KEM.667.320.
18. Yu, Y. Q., Guo, Y. L., Jiang, T., Jiang, K. Y., Guo, S. (2017). Laser sintering and post-processing of a walnut shell/Co-PES composite. *RSC Advances, 7(37),* 23176–23181. DOI 10.1039/C7RA00775B.
19. Idriss, A. I. B., Li, J., Wang, Y., Guo, Y., Adam, S. A. (2020). Selective laser sintering (SLS) and post-processing of prosopis chilensis/polyethersulfone composite (PCPC). *Materials, 13(13),* 3034. DOI 10.3390/ma13133034.
20. Idriss, A. I. B., Li, J., Guo, Y. L., Wang, Y. W., Li, X. D. (2020). Sintering quality and parameters optimization of sisal fiber/PES composite fabricated by selective laser sintering (SLS). *Journal of Thermoplastic Composite Materials, 15,* 1–15. DOI 10.1177/0892705720939179.
21. Kuo, C. C., Liu, L. C., Teng, W. F., Chang, H. Y., Chien, F. M. et al. (2016). Preparation of starch/acrylonitrile-butadiene-styrene copolymers (ABS) biomass alloys and their feasible evaluation for 3D printing applications. *Composites Part B: Engineering, 86,* 36–39. DOI 10.1016/j.compositesb.2015.10.005.
22. Sun, P., Zhang, L., Tao, S. (2019). Preparation of hybrid chitosan membranes by selective laser sintering for adsorption and catalysis. *Materials & Design, 173,* 107780. DOI 10.1016/j.matdes.2019.107780.
23. Qin, W. W., Zhang, L. (2012). The technology of comprehensive utilization of walnut shell in China. *Food Industry, 33(11),* 138–140.
24. Zeng, W. L., Guo, Y. L., Jiang, K. Y., Yu, Z. X., Liu, Y. et al. (2012). Laser intensity effect on mechanical properties of wood-plastic composite parts fabricated by selective laser sintering. *Journal of Thermoplastic Composite Materials, 26(1),* 125–136. DOI 10.1177/0892705712461520.
25. Zhao, D. J., Guo, Y. L., Song, W. L., Jiang, K. Y. (2015). Preparation and forming characteristics of bamboo powder/co-polyamide laser sintering composite materials. *Journal of Northeast Forestry University, 43,* 107–109, 115.
26. Yu, Y. Q., Guo, Y. L., Jiang, T., Li, J., Jiang, K. Y. et al. (2017). Study on the ingredient proportions and after-treating of laser sintering walnut shell composites. *Materials, 10(12),* 1381. DOI 10.3390/ma10121381.
27. Yu, Y. Q., Guo, Y. L., Jiang, T., Li, J., Jiang, K. Y. et al. (2018). Study on process and parameter optimization of selective laser sintering of walnut shell composite powder. *BioResources, 13,* 3017–3029. DOI 10.15376/biores.13.2.3017-3029.
28. Zhang, Z., Yao, X. X., Ge, P. (2020). Phase-field-model-based analysis of the effects of powder particle on porosities and densities in selective laser sintering additive manufacturing. *International Journal of Mechanical Sciences, 166,* 105230. DOI 10.1016/j.ijmecsci.2019.105230.